Correspondence

Power-Efficient Positioning for Visible Light Systems via Chance Constrained Optimization

The problem of minimizing total power consumption in light-emitting diode transmitters is investigated for achieving power efficient localization in a visible light communication and positioning system. A robust power allocation approach based on stochastic uncertainties is proposed for total power minimization in the presence of localization accuracy, power, and illumination constraints. Specifically, the power consumption minimization problem is formulated under a chance constraint on the probability of Cramér–Rao lower bound exceeding a tolerable limit, which is a computationally intractable constraint. The sphere bounding method is used to propose a safe convex approximation to this intractable constraint, which makes the resulting problem suitable for standard convex optimization tools. Numerical results demonstrate the advantages of the proposed robust solution over the nonrobust solution and uniform power allocation in the presence of stochastic uncertainty.

I. INTRODUCTION

Visible light communication (VLC) applications based on light-emitting diodes (LEDs) have become widespread in recent years due to the advances in LED technologies as well as their advantages over current wireless communication schemes [1]–[3]. VLC-based designs come into prominence not only because of their multipurpose utilization capability along with indoor illumination but also because they provide high data rates, low multipath fading, and no requirement of a licensed spectrum [4], [5].

Visible light positioning (VLP) systems, which involve the usage of visible light systems to accomplish localization tasks, have also become an intriguing area of research [6]–[8]. In VLP systems, the location of a VLC receiver can be estimated by utilizing the visible light signals transmitted by anchor nodes, which are LED transmitters with known locations [9].

Our main objective in this article is to design power efficient VLP systems by minimizing the total power consumption in LED transmitters while maintaining a desired level of localization performance under practical constraints. Although power and resource allocation has been investigated extensively for VLC systems (e.g., [10]–[16]), it has been

Manuscript received December 5, 2019; revised March 3, 2020; released for publication March 12, 2020. Date of publication March 20, 2020; date of current version October 9, 2020.

DOI. No. 10.1109/TAES.2020.2982304

Refereeing of this contribution was handled by J. Nichols.

Authors' addresses: Onurcan Yazar and Sinan Gezici are with the Department of Electrical and Electronics Engineering, Bilkent University, 06800 Ankara, Turkey, E-mail: (onurcan@ee.bilkent.edu.tr; gezici@ee.bilkent.edu.tr); Musa Furkan Keskin is with the Department of Electrical Engineering, Chalmers University of Technology, 41296 Gothenburg, Sweden, E-mail: (furkan@chalmers.se). *(Corresponding authors: Onurcan Yazar; Sinan Gezici.)*

considered only in a few studies for VLP systems [17]–[20]. In [17], an orthogonal frequency division multiple access (OFDMA) based visible light system with both communication and positioning capabilities is considered, and a power allocation algorithm is proposed to reduce the positioning error. The work in [18] focuses on a multiuser VLC and positioning (VLCP) system, and proposes a joint subcarrier and power allocation approach to maximize the sum rate under constraints on minimum data rates and localization accuracy of users. In [20], optimal and robust power allocation strategies are examined to improve localization performance of VLP systems and to address the problem of minimum power consumption in the presence of uncertainty modeled by deterministic norm-bounded errors. In this article, we propose the problem of minimum total power consumption for LED transmitters in a VLP system in which a stochastic approach is embraced in modeling the uncertainties in the localization parameters. To our knowledge, the total power minimization problem in the presence of stochastic uncertainty has not been considered before in the VLP literature, which is an important problem as the assumption of deterministically bounded errors may not be practical in general [21], [22].

The minimum total power consumption problem in the case of a deterministic norm-bounded uncertainty is solved in [20] through an upper constraint on the Cramér–Rao lower bound (CRLB) for the localization error, which yields a convex optimization problem. However, in the case of the stochastic uncertainty considered in this article, the fact that the unbounded parameter uncertainties come into the problem precludes the use of a worst case upper bound on the CRLB [21], [22]. For such a case, we propose to formulate the robust design problem as a *chance-constrained* optimization problem, in which a probabilistic constraint on the *localization accuracy outage probability* is established [23], [24]. We propose to solve this problem by proving that this probabilistic constraint can conservatively be approximated by a convex constraint via the *sphere bounding* method. This solution strategy is shown to satisfy any constraint on the localization accuracy outage probability as opposed to the nonrobust approach and the uniform power allocation strategy. The main contributions of this article over [20] are related to the consideration of a probabilistic constraint on the localization accuracy for the minimum total power consumption problem in a VLP system and the proposed solution approach based on the sphere bounding method.

II. SYSTEM MODEL

We consider a VLP setup in which the location of a VLC receiver is estimated by utilizing the signals sent by N_L LED transmitters. As the multipath fading effect is not significant in visible light systems compared to RF-based systems, only the line-of-sight path between each LED transmitter and the VLC receiver is considered [6], [25], [26]. The receiver is assumed to be able to process the signals sent by different LED transmitters individually by following a multiple access protocol (e.g., frequency division multiple access). Then, the received (electrical) signal at the output of the photodetector at the VLC receiver due to the signal transmitted by the ith LED transmitter can be modeled as [11], [27][1]

$$r_i(t) = \alpha_i R_p s_i(t-\tau_i) + \eta_i(t) \tag{1}$$

for $i \in \{1, \ldots, N_L\}$ and $t \in [T_{1,i}, T_{2,i}]$, where $T_{1,i}$ and $T_{2,i}$ are the starting and the ending time instants for VLC receiver's observation of the signal transmitted by the ith LED transmitter, α_i is the optical channel attenuation factor between the ith LED transmitter and the VLC receiver, R_p is the responsivity of the photodetector at the VLC receiver, $s_i(t)$ is the transmitted signal of the ith LED transmitter, τ_i is the time of arrival (TOA) of the signal arriving from the ith LED transmitter, and $\eta_i(t)$ are independent zero-mean additive white Gaussian noise processes each having a spectral density level of σ^2 (with the independence stemming from the multiple access protocol).

The TOA in (1) can be determined by

$$\tau_i = \frac{||\boldsymbol{l}_{\mathrm{r}} - \boldsymbol{l}_{\mathrm{t}}^i||}{c} + \delta_i \tag{2}$$

where the positions of the VLC receiver and the ith LED transmitter are denoted by $\boldsymbol{l}_{\mathrm{r}} = [l_{r,1}\ l_{r,2}\ l_{r,3}]^T$ and $\boldsymbol{l}_{\mathrm{t}}^i = [l_{t,1}^i\ l_{t,2}^i\ l_{t,3}^i]^T$, respectively, c denotes the speed of light, $||\cdot||$ specifies the Euclidean norm, and δ_i stands for the clock offset between the VLC receiver and the ith LED transmitter, which is equal to zero in synchronous systems and regarded as an unknown parameter in asynchronous systems [27].

The optical channel attenuation factors α_i given in (1) can be expressed through the Lambertian model as [28]

$$\alpha_i = \frac{S(m_i+1)(\boldsymbol{l}_{\mathrm{t}}^i - \boldsymbol{l}_{\mathrm{r}})^T \boldsymbol{n}_{\mathrm{r}}}{2\pi \left((\boldsymbol{l}_{\mathrm{r}} - \boldsymbol{l}_{\mathrm{t}}^i)^T \boldsymbol{n}_{\mathrm{t}}^i\right)^{-m_i} ||\boldsymbol{l}_{\mathrm{r}} - \boldsymbol{l}_{\mathrm{t}}^i||^{m_i+3}} \tag{3}$$

where S is the area of the photodetector at the VLC receiver, m_i stands for the Lambertian order for the ith LED, and $\boldsymbol{n}_{\mathrm{r}} = [n_{r,1}\ n_{r,2}\ n_{r,3}]^T$ and $\boldsymbol{n}_{\mathrm{t}}^i = [n_{t,1}^i\ n_{t,2}^i\ n_{t,3}^i]^T$ correspond to the orientation vectors for the VLC receiver and the ith LED transmitter, respectively. In this configuration, it is assumed that parameters S and $\boldsymbol{n}_{\mathrm{r}}$ are known by the VLC receiver (e.g., via measurements from a gyroscope) and the parameters related to the LED transmitters (i.e., m_i, $\boldsymbol{l}_{\mathrm{t}}^i$, and $\boldsymbol{n}_{\mathrm{t}}^i$) can be acquired by the VLC receiver through communications with each of the LED transmitters.

III. PROBLEM FORMULATION AND PROPOSED APPROACH

In this section, we first formulate a robust total power minimization problem for VLP systems under a chance constraint related to the localization accuracy of the VLC receiver. Then, we apply the sphere bounding method to provide a low-complexity solution to the proposed problem.

[1]The signal model in (1) is in compliance with [11, eq. (3)] for the case of single-color LEDs.

A. Assessment of Localization Performance

In order to quantify the localization performance of the VLP system, the CRLB for the location estimation error is chosen as the performance metric. The main motivations behind the use of the CRLB metric are that the maximum-likelihood estimator achieves a very close performance to the CRLB at high signal-to-noise ratios and that CRLB expressions commonly facilitate theoretical investigations and analyses [20].

Among other factors, the CRLB is related to the transmitted signals $s_i(t)$ utilized in the localization of the VLC receiver. As in [20], the transmitted signals can be represented in terms of base signals $\widetilde{s}_i(t)$ as

$$s_i(t) = \sqrt{P_i}\,\widetilde{s}_i(t) \tag{4}$$

for $i \in \{1, \ldots, N_L\}$, where the nonnegative base signal represents the normalized version of the transmitted signal such that it has a unit power, i.e., it satisfies $\int_0^{T_{s,i}} (\widetilde{s}_i(t))^2 dt = T_{s,i}$, where $T_{s,i}$ denotes the duration of the transmitted signal. In other words, in this configuration, P_i indicates the electrical transmit power of the ith LED transmitter. Then, we define

$$\mathbf{p} \triangleq \left[P_1 \cdots P_{N_L}\right]^T \tag{5}$$

which is used as the main optimization variable for the minimum total power consumption problem. As shown in (4), our power optimization framework relies on scaling the nonnegative base signals $\widetilde{s}_i(t)$ by parameters $\sqrt{P_i}$, which implies that adjusting $\mathbf{p}$ in (5) affects both the dc and ac parts of the LED signals.

The CRLB on the variance of any unbiased estimator $\hat{\boldsymbol{l}}_{\rm r}$ for the VLC receiver location $\boldsymbol{l}_{\rm r}$ is expressed as [27]

$$\mathbb{E}\left\{||\hat{\boldsymbol{l}}_{\rm r} - \boldsymbol{l}_{\rm r}||^2\right\} \geq \text{trace}\left\{\mathbf{J}^{-1}(\mathbf{p})\right\} \tag{6}$$

where $\mathbf{J}(\mathbf{p})$ is the Fisher information matrix (FIM), which is computed by [20]

$$\mathbf{J}(\mathbf{p}) = (\mathbf{I}_3 \otimes \mathbf{p})^T \boldsymbol{\Gamma}\,. \tag{7}$$

In (7), $\mathbf{I}_3$ is a 3×3 identity matrix, $\otimes$ denotes the Kronecker product, and

$$\boldsymbol{\Gamma} \triangleq \begin{bmatrix} \boldsymbol{\gamma}_{1,1} & \boldsymbol{\gamma}_{1,2} & \boldsymbol{\gamma}_{1,3} \\ \boldsymbol{\gamma}_{2,1} & \boldsymbol{\gamma}_{2,2} & \boldsymbol{\gamma}_{2,3} \\ \boldsymbol{\gamma}_{3,1} & \boldsymbol{\gamma}_{3,2} & \boldsymbol{\gamma}_{3,3} \end{bmatrix} \in \mathbb{R}^{3N_L \times 3} \tag{8}$$

with

$$\boldsymbol{\gamma}_{k_1,k_2} \triangleq \left[\gamma_{k_1,k_2}^{(1)} \ \ldots \ \gamma_{k_1,k_2}^{(N_L)}\right]^T \in \mathbb{R}^{N_L} \tag{9}$$

for $k_1, k_2 \in \{1, 2, 3\}$ [20]. $\gamma_{k_1,k_2}^{(i)}$ in (9) is as described in [20, Appendix A], which for convenience is also stated as follows:

$$\gamma_{k_1,k_2}^{(i)} = \begin{cases} \gamma_{k_1,k_2}^{(i),\rm syn}, & \text{if synchronous VLP system} \\ \gamma_{k_1,k_2}^{(i),\rm asy}, & \text{if asynchronous VLP system} \end{cases}$$

$$\gamma_{k_1,k_2}^{(i),\rm syn} \triangleq \frac{R_p^2}{\sigma^2}\left(E_2^i \frac{\partial \alpha_i}{\partial l_{{\rm r},k_1}} \frac{\partial \alpha_i}{\partial l_{{\rm r},k_2}} + E_1^i \alpha_i^2 \frac{\partial \tau_i}{\partial l_{{\rm r},k_1}} \frac{\partial \tau_i}{\partial l_{{\rm r},k_2}} \right.$$
$$\left. - E_3^i \alpha_i \left(\frac{\partial \alpha_i}{\partial l_{{\rm r},k_1}} \frac{\partial \tau_i}{\partial l_{{\rm r},k_2}} + \frac{\partial \tau_i}{\partial l_{{\rm r},k_1}} \frac{\partial \alpha_i}{\partial l_{{\rm r},k_2}}\right)\right)$$

$$\gamma_{k_1,k_2}^{(i),\rm asy} \triangleq \frac{R_p^2}{\sigma^2}\left(E_2^i - \frac{(E_3^i)^2}{E_1^i}\right) \frac{\partial \alpha_i}{\partial l_{{\rm r},k_1}} \frac{\partial \alpha_i}{\partial l_{{\rm r},k_2}}$$

$$E_1^i \triangleq \int_0^{T_{s,i}} \left(\widetilde{s}_i'(t)\right)^2 dt\,, \quad E_2^i \triangleq \int_0^{T_{s,i}} \left(\widetilde{s}_i(t)\right)^2 dt$$

$$E_3^i \triangleq \int_0^{T_{s,i}} \widetilde{s}_i(t) \widetilde{s}_i'(t) dt\,, \quad \frac{\partial \tau_i}{\partial l_{{\rm r},k}} = \frac{l_{{\rm r},k} - l_{{\rm t},k}^i}{c\|\boldsymbol{l}_{\rm r} - \boldsymbol{l}_{\rm t}^i\|}$$

$$\frac{\partial \alpha_i}{\partial l_{{\rm r},k}} = -\frac{(m_i+1)S}{2\pi}\left(\frac{\left((\boldsymbol{l}_{\rm r} - \boldsymbol{l}_{\rm t}^i)^T \boldsymbol{n}_{\rm t}^i\right)^{m_i - 1}}{\|\boldsymbol{l}_{\rm r} - \boldsymbol{l}_{\rm t}^i\|^{m_i+3}} \right.$$
$$\times \left(m_i\, n_{{\rm t},k}^i \left(\boldsymbol{l}_{\rm r} - \boldsymbol{l}_{\rm t}^i\right)^T \boldsymbol{n}_{\rm r} + n_{{\rm r},k} \left(\boldsymbol{l}_{\rm r} - \boldsymbol{l}_{\rm t}^i\right)^T \boldsymbol{n}_{\rm t}^i\right)$$
$$- \frac{(m_i+3)(l_{{\rm r},k} - l_{{\rm t},k}^i)}{\|\boldsymbol{l}_{\rm r} - \boldsymbol{l}_{\rm t}^i\|^{m_i+5}}$$
$$\left. \times \left((\boldsymbol{l}_{\rm r} - \boldsymbol{l}_{\rm t}^i)^T \boldsymbol{n}_{\rm t}^i\right)^{m_i} (\boldsymbol{l}_{\rm r} - \boldsymbol{l}_{\rm t}^i)^T \boldsymbol{n}_{\rm r}\right)$$

where $\widetilde{s}_i'(t)$ denotes the derivative of $\widetilde{s}_i(t)$.

REMARK 1 From the preceding expressions, it is noted that, for a given power vector $\mathbf{p}$, the CRLB is determined by matrix $\boldsymbol{\Gamma}$, which depends on the VLP system parameters, consisting of R_p, S, σ^2, $\boldsymbol{l}_{\rm r}$, $\boldsymbol{n}_{\rm r}$, $\boldsymbol{l}_{\rm t}^i$, $\boldsymbol{n}_{\rm t}^i$, m_i, E_1^i, E_2^i, and E_3^i for $i \in \{1, \ldots, N_L\}$. In general, the knowledge of the receiver related parameters except for $\boldsymbol{l}_{\rm r}$, namely, R_p, S, σ^2, and $\boldsymbol{n}_{\rm r}$, can be available at the VLC receiver or obtained by it via previous observations or sensor (e.g., gyroscope) measurements. Similarly, the knowledge of the transmitter related parameters, $\boldsymbol{l}_{\rm t}^i$, $\boldsymbol{n}_{\rm t}^i$, m_i, E_1^i, E_2^i, and E_3^i, is available at the LED transmitters. Since the knowledge of some system parameters (e.g., $\boldsymbol{n}_{\rm r}$) may be imperfect and $\boldsymbol{l}_{\rm r}$ is unknown in general, it is not possible to know $\boldsymbol{\Gamma}$ perfectly. Hence, a robust approach should be taken by employing a suitable uncertainty model for the information about $\boldsymbol{\Gamma}$. ■

B. Practical Constraints on LED Powers

Before the formulation of the optimization problem, the constraint sets on the LED powers should be specified. These limitations are due to practical concerns, such as hardware requirements and desired ambient illumination levels.

1) Individual bounds on each of the allocated LED powers exist for guaranteeing the operation of each LED in the linear region so as to provide efficient optical energy conversion and also to prevent self-heating resulting from high currents flowing through the LEDs. Thus, the constraint set $\mathcal{P}_1$ in [20, eq. (12)] must be considered, which is stated as follows:

$$\mathcal{P}_1 \triangleq \{\mathbf{p} \in \mathbb{R}^{N_{\rm L}} : \mathbf{p}_{\rm lb} \preceq \mathbf{p} \preceq \mathbf{p}_{\rm ub}\} \tag{10}$$

where $\mathbf{p}_{\rm lb} \in \mathbb{R}^{N_{\rm L}}$ and $\mathbf{p}_{\rm ub} \in \mathbb{R}^{N_{\rm L}}$ represent, respectively, the lower and upper bounds on $\mathbf{p}$ in (5).

2) The fact that VLP systems are used for illumination purposes in indoor scenarios may necessitate particular locations over the region to have illumination limitations. Therefore, we have the constraint set $\mathcal{P}_3$ specified in [20, eq. (17)], which is expressed as

$$\mathcal{P}_3 \triangleq \{\mathbf{p} \in \mathbb{R}^{N_\mathrm{L}} : \mathcal{I}_\mathrm{ind}(\mathbf{x}_\ell, \mathbf{p}) \geq \widetilde{\mathcal{I}}_\ell,\ \ell = 1, \ldots, L\} \tag{11}$$

with L denoting the number of locations at which the illuminance constraint should be satisfied and $\widetilde{\mathcal{I}}_\ell$ being the illuminance constraint for location $\mathbf{x}_\ell$. In addition, $\mathcal{I}_\mathrm{ind}(\mathbf{x}_\ell, \mathbf{p})$ in (11) is given by [20]

$$\mathcal{I}_\mathrm{ind}(\mathbf{x}_\ell, \mathbf{p}) = \sum_{i=1}^{N_\mathrm{L}} \sqrt{P_i}\,\phi_i(\mathbf{x}_\ell)$$

with

$$\phi_i(\mathbf{x}) = \frac{(m_i+1)\kappa_i \widetilde{E}_i^\mathrm{opt}\left[(\mathbf{x} - \boldsymbol{l}_\mathrm{t}^i)^T \boldsymbol{n}_\mathrm{t}^i\right]^{m_i} (l_{\mathrm{t},3}^i - x_3)}{2\pi\,\|\mathbf{x} - \boldsymbol{l}_\mathrm{t}^i\|^{m_i+3}} \tag{12}$$

where $\widetilde{E}_i^\mathrm{opt} \triangleq \int_0^{T_{s,i}} \widetilde{s}_i(t)dt \big/ T_{s,i}$ and κ_i represents the luminous efficacy (lm/W) of the ith LED [29]. It is noted that the illumination constraints are related to the dc levels of the transmitted signals.

3) In some scenarios, an additional average illuminance constraint over a certain region (e.g., the entire indoor region) may exist. In order to handle such situations, we induce the constraint set $\mathcal{P}_4$ in [20, eq. (19)], which can be stated as

$$\mathcal{P}_4 \triangleq \left\{\mathbf{p} \in \mathbb{R}^{N_\mathrm{L}} : \sum_{i=1}^{N_\mathrm{L}} \frac{\sqrt{P_i}}{|\mathcal{A}|} \int_\mathcal{A} \phi_i(\mathbf{x}) d\mathbf{x} \geq \widetilde{\mathcal{I}}_\mathrm{avg}\right\} \tag{13}$$

where $\mathcal{A}$ denotes the region, $|\mathcal{A}|$ is the volume of $\mathcal{A}$, $\phi_i(\mathbf{x})$ is as in (12), and $\widetilde{\mathcal{I}}_\mathrm{avg}$ represents the average illuminance constraint.

C. Robust Minimization of Total Power Consumption via Chance Constrained Programming

The aim is to perform optimal power allocation among the LED transmitters in order to minimize their total power consumption under a constraint on the localization accuracy of the VLC receiver as well as the practical constraints in Section III-B. This power allocation operation is performed by a central controller (e.g., a microcontroller) that sets the parameters of the LED transmitters [19]. Since the knowledge of the system parameters that determine $\mathbf{\Gamma}$ (hence, the CRLB) may not be available at the central controller (Remark 1), the power allocation should be performed in the presence of imperfect knowledge. Therefore, a robust constraint should be considered for the localization accuracy of the VLC receiver. If upper and lower bounds on the error related to each system parameter are known, a deterministic norm-bounded uncertainty model as in [20] can be employed for $\mathbf{\Gamma}$. However, such knowledge may not always be available due to stochastic nature of error sources in measuring some parameters. As an alternative approach, we propose a stochastic uncertainty model in this article. Namely, we model the uncertainty in the measurement of the actual localization parameter matrix $\mathbf{\Gamma}$ by considering the measured value of $\mathbf{\Gamma}$ as $\widetilde{\mathbf{\Gamma}} = \mathbf{\Gamma} + \mathbf{\Delta\Gamma}$, where $\mathbf{\Delta\Gamma}$ represents the stochastic error matrix. The fact that the measured matrix $\widetilde{\mathbf{\Gamma}}$ is obtained as a result of the noisy estimates of the true matrix $\mathbf{\Gamma}$ leads us to consider the error matrix $\mathbf{\Delta\Gamma}$ having a certain probabilistic structure [30]–[33]. Similar to RF [23], [30] and visible light [21], [22] based models, we can model the free entries[2] in $\mathbf{\Delta\Gamma} \in \mathbb{R}^{3N_L\times 3}$ as independent and identically distributed zero-mean Gaussian random variables with variance σ_e^2, i.e., $\Delta\Gamma_{jk} \sim \mathcal{N}(0, \sigma_e^2)$, where $\Delta\Gamma_{jk}$ is the (j,k)th entry in $\mathbf{\Delta\Gamma}$ for $(j,k) \in \{1,\ldots,3N_L\} \times \{1,2,3\}$. This can alternatively be stated as

$$\begin{bmatrix} \mathbf{v}_d(\mathbf{\Delta\Gamma}) \\ \mathbf{v}_{od}(\mathbf{\Delta\Gamma}) \end{bmatrix} \sim \mathcal{N}\left(\begin{bmatrix} \mathbf{0} \\ \mathbf{0} \end{bmatrix}, \begin{bmatrix} \sigma_e^2 \mathbf{I}_{3N_L} & \mathbf{0} \\ \mathbf{0} & \sigma_e^2 \mathbf{I}_{3N_L} \end{bmatrix}\right) \tag{14}$$

where $\mathbf{v}_d(\mathbf{\Gamma})$ and $\mathbf{v}_{od}(\mathbf{\Gamma})$ (both $\mathbb{R}^{3N_L\times 3} \to \mathbb{R}^{3N_L\times 1}$) denote the vectorization operators to stack the diagonal (i.e., $\boldsymbol{\gamma}_{j,j}$ for $j \in \{1,2,3\}$) and the off-diagonal (i.e., $\boldsymbol{\gamma}_{j,k}$ for $j \neq k$ and $j,k \in \{1,2,3\}$) columns of any matrix $\mathbf{\Gamma} \in \mathbb{R}^{3N_L\times 3}$ having the structure in (8).

REMARK 2 The use of the Gaussian error model in (14), which is also employed in [21]–[23], [30] can be justified by the fact that the Gaussian distribution corresponds to the worst case scenario as it maximizes the differential entropy for a given mean and variance. Hence, it leads to a conservative (robust) approach. ■

REMARK 3 Referring to Remark 1, the transmitter-related parameters, $\boldsymbol{l}_\mathrm{t}^i, \boldsymbol{n}_\mathrm{t}^i, m_i, E_1^i, E_2^i$, and E_3^i, are already available at the central controller, and the receiver-related parameters, R_p, S, σ^2, and $\boldsymbol{n}_\mathrm{r}$, can be sent to the central controller via the uplink (e.g., via WiFi or infrared links [17] and [19]). In addition, the position estimate at the VLC receiver can be sent to the central controller regularly so that it can have imperfect knowledge of $\boldsymbol{l}_\mathrm{r}$ for the power allocation operation in the next cycle. Overall, the uncertainty in the knowledge of $\mathbf{\Gamma}$ is caused by many factors, such as the errors in measuring parameters, the errors during communications from the VLC receiver to the central controller, and the dynamics of the VLC receiver. ■

As the Gaussian distributed errors $\Delta\Gamma_{jk}$ are unbounded, a worst case constraint on the CRLB cannot be imposed. Therefore, in order to handle such uncertainties, we propose a *chance-constrained programming* based optimization approach, where we introduce an upper constraint ζ on the probability that the CRLB exceeds a certain level ϵ. This constraint can be stated as

$$\mathrm{Prob}_{\mathbf{\Delta\Gamma}}\left\{\mathrm{trace}\{\mathbf{J}^{-1}(\mathbf{p})\} \leq \epsilon\right\} \geq 1 - \zeta \tag{15}$$

where $\mathbf{\Delta\Gamma}$ has the distribution specified in (14) and ϵ represents the threshold value that the CRLB is expected

[2]It is noted that $\mathbf{\Gamma}$ in (8) contains $6N_L$ free entries as $\boldsymbol{\gamma}_{k_1,k_2} = \boldsymbol{\gamma}_{k_2,k_1}$.

to exceed only by a maximum chance of $\zeta \in (0, 1)$, which is called the *localization accuracy outage probability*. (For notational simplicity, we omit subscript $\mathbf{\Delta\Gamma}$ in (15) in the remainder of the manuscript.) The minimum total power consumption problem with the localization accuracy outage probability constraint can then be proposed as

$$\underset{\mathbf{p}}{\text{minimize}} \quad \mathbf{1}^T\mathbf{p} \tag{16a}$$

$$\text{subject to} \quad \text{Prob}\left\{\text{trace}\{\mathbf{J}^{-1}(\mathbf{p})\right\} \leq \epsilon\} \geq 1-\zeta \tag{16b}$$

$$\mathbf{p} \in \mathcal{P} \tag{16c}$$

where $\mathbf{J}(\mathbf{p}) = (\mathbf{I}_3 \otimes \mathbf{p})^T(\widetilde{\mathbf{\Gamma}} - \mathbf{\Delta\Gamma})$ is the FIM given in (7) and $\mathcal{P} \triangleq \mathcal{P}_1 \cap \mathcal{P}_3 \cap \mathcal{P}_4$ stands for the practical LED power constraints mentioned in Section III-B [please see (10), (11), and (13)].

Since the chance constraint in (16b) is not computationally tractable, we resort to the *sphere bounding* method to derive a tractable convex constraint that provides a safe approximation to (16b) in the sense that any point satisfying the new constraint also satisfies (16b) [33]. The following proposition presents a worst case type deterministic condition under which the probabilistic constraint (16b) always holds.

Proposition 1 Let $\mathcal{B} \triangleq \{\mathbf{\Psi} \in \mathbb{R}^{3N_L \times 3} : ||\mathbf{\Psi}|| \leq \xi\}$, where $||\cdot||$ denotes the matrix spectral norm and ξ is defined as

$$\xi \triangleq \sigma_e \sqrt{3\Phi^{-1}_{\chi^2_{3N_L}}\left(\sqrt{1-\zeta}\right)} \tag{17}$$

with $\Phi^{-1}_{\chi^2_{3N_L}}(\cdot)$ denoting the inverse cumulative distribution function (CDF) of a chi-squared random variable with $3N_L$ degrees of freedom. Then, the following implication holds true:

$$\begin{aligned}&\text{trace}\{[(\mathbf{I}_3 \otimes \mathbf{p})^T(\widetilde{\mathbf{\Gamma}} - \mathbf{\Psi})]^{-1}\} \leq \epsilon \quad \forall \mathbf{\Psi} \in \mathcal{B}\\ &\Longrightarrow \text{Prob}\left\{\text{trace}\{[(\mathbf{I}_3 \otimes \mathbf{p})^T(\widetilde{\mathbf{\Gamma}} - \mathbf{\Delta\Gamma})]^{-1}\} \leq \epsilon\right\} \geq 1-\zeta.\end{aligned} \tag{18}$$

Proof We define new sets $\mathcal{B}_s$ and $\widetilde{\mathcal{B}}$ as

$$\mathcal{B}_s \triangleq \left\{\mathbf{\Psi} \in \mathbb{R}^{3N_L \times 3} : \ ||\mathbf{v}_d(\mathbf{\Psi})||_2 \leq \frac{\xi}{\sqrt{3}}, ||\mathbf{v}_{od}(\mathbf{\Psi})||_2 \leq \frac{\xi}{\sqrt{3}}\right\} \tag{19}$$

and

$$\widetilde{\mathcal{B}} \triangleq \{\mathbf{\Psi} \in \mathbb{R}^{3N_L \times 3} : ||\mathbf{\Psi}||_F \leq \xi\} \tag{20}$$

where $||\cdot||_F$ denotes the Frobenius norm. First, we note that

$$\begin{aligned}\text{Prob}\{\mathbf{\Delta\Gamma} \in \mathcal{B}_s\} &= \text{Prob}\left\{||\mathbf{v}_d(\mathbf{\Delta\Gamma})||_2 \leq \frac{\xi}{\sqrt{3}}\right\}\\ &\times \text{Prob}\left\{||\mathbf{v}_{od}(\mathbf{\Delta\Gamma})||_2 \leq \frac{\xi}{\sqrt{3}}\right\} &\text{(21a)}\\ &= \left[\text{Prob}\left\{(||\mathbf{v}_d(\mathbf{\Delta\Gamma})||_2/\sigma_e)^2 \leq \Phi^{-1}_{\chi^2_{3N_L}}\left(\sqrt{1-\zeta}\right)\right\}\right]^2 &\text{(21b)}\\ &= 1-\zeta &\text{(21c)}\end{aligned}$$

where (21a) follows from (19) and (14), (21b) is based on (17), and (21c) is due to (14) and the definition of $\Phi^{-1}_{\chi^2_{3N_L}}(\cdot)$. Now, assume that the left-hand side (LHS) of (18) is satisfied. Since $\mathcal{B}_s \subseteq \widetilde{\mathcal{B}}$ via (19) and (20), and $\widetilde{\mathcal{B}} \subseteq \mathcal{B}$ via $||\mathbf{\Psi}|| \leq ||\mathbf{\Psi}||_F$, we obtain

$$\text{trace}\left\{\left[(\mathbf{I}_3 \otimes \mathbf{p})^T\left(\widetilde{\mathbf{\Gamma}} - \mathbf{\Psi}\right)\right]^{-1}\right\} \leq \epsilon \quad \forall \mathbf{\Psi} \in \mathcal{B}_s. \tag{22}$$

Then, we have

$$\begin{aligned}&\text{Prob}\left\{\text{trace}\left\{\left[(\mathbf{I}_3 \otimes \mathbf{p})^T(\widetilde{\mathbf{\Gamma}} - \mathbf{\Delta\Gamma})\right]^{-1}\right\} \leq \epsilon\right\}\\ &\geq \text{Prob}\{\mathbf{\Delta\Gamma} \in \mathcal{B}_s\}\end{aligned} \tag{23}$$

which yields the desired result in (18) via (21). ■

Based on the implication in (18), the constraint (16b) can be replaced by the LHS of (18), which can be transformed into a set of linear matrix inequality (LMI) constraints. Proposition 2 asserts to construct a convex optimization problem that constitutes a conservative tractable approximation of the original problem in (16).

Proposition 2 The chance constrained problem in (16) can safely be approximated through the following convex optimization problem (i.e., any feasible point of (24) is feasible for (16)):

$$\underset{\mathbf{p},\mathbf{H},s,\mu}{\text{minimize}} \quad \mathbf{1}^T\mathbf{p} \tag{24a}$$

$$\text{subject to} \quad \text{trace}\{\mathbf{H}\} \leq \epsilon - Ds \tag{24b}$$

$$\mathbf{\Phi}(\mathbf{p}, \mathbf{H}, s, \mu) \succeq 0, \mathbf{H} \succeq 0, \mu \geq 0 \tag{24c}$$

$$\mathbf{p} \in \mathcal{P} \tag{24d}$$

where D stands for the dimension of localization; $\mathbf{H}$, s, and μ are auxiliary variables; and

$$\mathbf{\Phi}(\mathbf{p}, \mathbf{H}, s, \mu) \triangleq \begin{bmatrix}\mathbf{H} + s\mathbf{I} & \mathbf{I} & \mathbf{0}\\ \mathbf{I} & (\mathbf{I}_3 \otimes \mathbf{p})^T\widetilde{\mathbf{\Gamma}} - \mu\mathbf{I} & -\frac{\xi}{2}(\mathbf{I}_3 \otimes \mathbf{p})^T\\ \mathbf{0} & -\frac{\xi}{2}(\mathbf{I}_3 \otimes \mathbf{p}) & \mu\mathbf{I}\end{bmatrix} \tag{25}$$

with ξ being defined in (17).

Proof Following the same steps as in the proof of [20, Proposition 3], the LHS of (18) can be shown to be equivalent to the LMI constraints in (24b)–(24d). Hence, according to Proposition 1, the feasible region of (24) is contained entirely in the feasible region of (16). ■

Based on Proposition 2, the convex optimization problem in (24) can be solved to perform power efficient localization in VLP systems by satisfying the chance constraint in (16b) as well as the practical constraints in (16c).

IV. NUMERICAL RESULTS

In this section, we present a numerical example to investigate the performance of the proposed approach for the chance-constrained minimum total power consumption problem. We consider an asynchronous VLP setup in a room of size $10 \times 10 \times 5\,\text{m}^3$ with $N_L = 4$ LED transmitters and a VLC receiver whose locations and orientations are

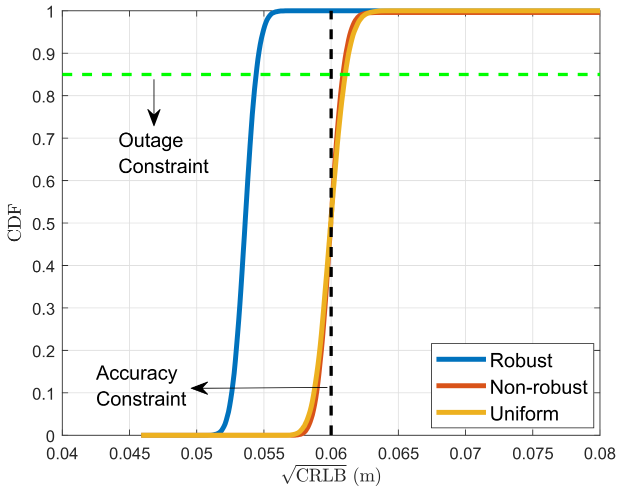

(a)

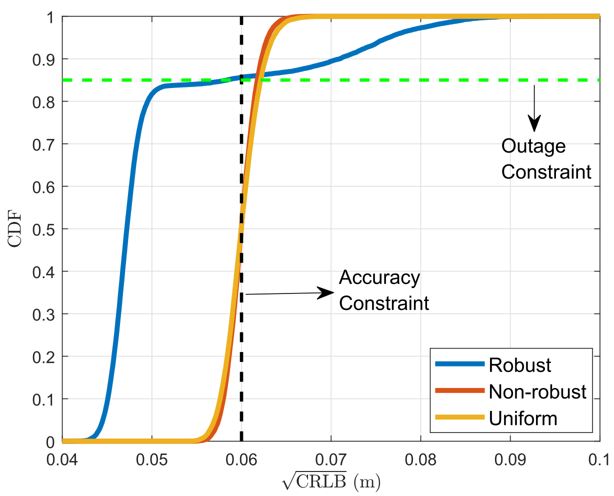

(b)

Fig. 1. CDF of localization CRLBs achieved by robust, nonrobust, and uniform strategies in case of stochastic uncertainty, where the accuracy constraint on CRLB in (16) is set to $\sqrt{\epsilon} = 0.06$ m, the outage probability constraint is $\zeta = 0.15$, and two different noise variances (a) $\sigma_e^2 = 10^{-4}$ and (b) $\sigma_e^2 = 4 \times 10^{-4}$ are considered.

as specified in [20, Table I]. The scaled version of the signal transmitted from the ith LED transmitter is modeled as $\widetilde{s}_i(t) = \frac{2}{3}(1 - \cos(2\pi t/T_{s,i}))(1 + \cos(2\pi f_{c,i} t))$ for $i = 1, \ldots, N_L$ and $t \in [0, T_{s,i}]$, where the pulse width $T_{s,i}$ and the center frequency $f_{c,i}$ along with the other simulation parameters are as provided in [20, Table II]. The robust strategy illustrated in Fig. 1 refers to the solution of the convex approximation in (24). This strategy is compared with the nonrobust strategy of solving the worst case accuracy constrained optimization problem using the noisy measurement $\widetilde{\mathbf{\Gamma}}$, which can be formulated as [20]

$$\underset{\mathbf{p}}{\text{minimize}} \quad \mathbf{1}^T \mathbf{p} \tag{26a}$$

$$\text{subject to} \quad \operatorname{trace}\left\{\left[(\mathbf{I}_3 \otimes \mathbf{p})^T \widetilde{\mathbf{\Gamma}}\right]^{-1}\right\} \leq \epsilon \tag{26b}$$

$$\mathbf{p} \in \mathcal{P} \tag{26c}$$

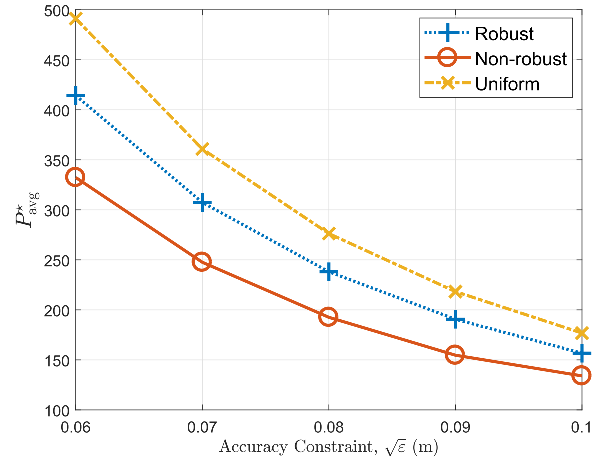

Fig. 2. Optimal value of (16a) divided by N_L (P^*_{avg}) versus accuracy constraint $\sqrt{\epsilon}$ for robust, nonrobust, and uniform power allocation strategies, where the outage constraint is $\zeta = 0.15$ and the noise variance is $\sigma_e^2 = 10^{-4}$.

and also with the uniform power allocation strategy of

$$P_i = \operatorname{trace}\left\{\left[(\mathbf{I}_3 \otimes \mathbf{1})^T \widetilde{\mathbf{\Gamma}}\right]^{-1}\right\} / \epsilon \tag{27}$$

for $i \in \{1, \ldots, N_L\}$.

Fig. 1(a) and (b) shows the CDF of the CRLB for different noise variances in (14), namely $\sigma_e^2 = 10^{-4}$ and $\sigma_e^2 = 4 \times 10^{-4}$, respectively, where the outage probability limit in (16) is set to $\zeta = 0.15$. We observe that the proposed robust strategy satisfies the probabilistic constraint in (16), i.e., it guarantees the specified accuracy level ϵ for $100(1 - \zeta)\%$ of the realizations. On the other hand, the other two approaches fail to satisfy the chance constraint in (16) as they disregard the probabilistic uncertainty in $\mathbf{\Gamma}$. In addition, the robust strategy tends to oversatisfy the probabilistic constraint as σ_e decreases, which indicates that the approximation in Proposition 2 becomes tighter for higher levels of uncertainty.

Fig. 2 illustrates the average power of the LEDs versus the accuracy constraint $\sqrt{\epsilon}$ for the robust, nonrobust, and uniform power allocation strategies, where $\zeta = 0.15$ and $\sigma_e^2 = 10^{-4}$. It is observed that the uniform power allocation strategy consumes the highest transmit powers. Also, it is noted that the relative performance gain of the proposed robust strategy is achieved at the cost of higher transmit powers than those in the nonrobust approach. However, it should be emphasized that the robust strategy provides a solid theoretical guarantee for satisfying the chance constraint in (16) unlike the nonrobust and uniform power allocation approaches.

V. CONCLUDING REMARKS

In this article, the minimization of total power consumption in LED transmitters in a VLP system has been considered via a chance-constrained programming approach. We have formulated the problem with a stochastic uncertainty model for the localization parameters. This yields an optimization problem having an intractable nonconvex constraint related to the probability that the localization CRLB exceeds a certain level as well as constraints on LED powers regarding the hardware requirements and the illumination task of the VLP system. We have demonstrated that the sphere bounding method can be applied to approximate the nonconvex constraint with a convex one, which facilitates the solution of the minimum total power consumption problem via standard convex optimization tools. The numerical results show that via the proposed robust approach, constraints on the localization accuracy outage probability can always be satisfied as opposed to the uniform and nonrobust strategies, with a power consumption level in between the two.

ONURCAN YAZAR
Bilkent University, Ankara, Turkey

MUSA FURKAN KESKIN, *Member, IEEE*
Chalmers University of Technology,
Gothenburg, Sweden

SINAN GEZICI, *Senior Member, IEEE*
Bilkent University, Ankara, Turkey

REFERENCES

[1] D. Karunatilaka, F. Zafar, V. Kalavally, and R. Parthiban
LED based indoor visible light communications: State of the art
IEEE Commun. Surv. Tut., vol. 17, no. 3, pp. 1649–1678, Jul.–Sep. 2015.

[2] H. Elgala, R. Mesleh, and H. Haas
Indoor optical wireless communication: Potential and state-of-the-art
IEEE Commun. Mag., vol. 49, no. 9, pp. 56–62, Sep. 2011.

[3] D. N. Amanor, W. W. Edmonson, and F. Afghah
Intersatellite communication system based on visible light
IEEE Trans. Aerosp. Electron. Syst., vol. 54, no. 6, pp. 2888–2899, Dec. 2018.

[4] A. Jovicic, J. Li, and T. Richardson
Visible light communication: Opportunities, challenges and the path to market
IEEE Commun. Mag., vol. 51, no. 12, pp. 26–32, Dec. 2013.

[5] L. Grobe *et al.*
High-speed visible light communication systems
IEEE Commun. Mag., vol. 51, no. 12, pp. 60–66, Dec. 2013.

[6] J. Armstrong, Y. Sekercioglu, and A. Nelid
Visible light positioning: A roadmap for international standardization
IEEE Commun. Mag., vol. 51, no. 12, pp. 68–73, Dec. 2013.

[7] N. U. Hassan, A. Naeem, M. A. Pasha, T. Jadoon, and C. Yuen
Indoor positioning using visible LED lights: A survey
ACM Comput. Surv., vol. 48, no. 2, pp. 1–32, Nov. 2015.

[8] B. Zhou, A. Liu, and V. Lau
Performance limits of visible light-based user position and orientation estimation using received signal strength under NLOS propagation
IEEE Trans. Wireless Commun., vol. 18, no. 11, pp. 5227–5241, Nov. 2019.

[9] M. F. Keskin, A. D. Sezer, and S. Gezici
Localization via visible light systems
Proc. IEEE, vol. 106, no. 6, pp. 1063–1088, Jun. 2018.

[10] D. Bykhovsky and S. Arnon
Multiple access resource allocation in visible light communication systems
J. Lightw. Technol., vol. 32, no. 8, pp. 1594–1600, Apr. 2014.

[11] C. Gong, S. Li, Q. Gao, and Z. Xu
Power and rate optimization for visible light communication system with lighting constraints
IEEE Trans. Signal Process., vol. 63, no. 16, pp. 4245–4256, Aug. 2015.

[12] X. Ling, J. Wang, X. Liang, Z. Ding, and C. Zhao
Offset and power optimization for DCO-OFDM in visible light communication systems
IEEE Trans. Signal Process., vol. 64, no. 2, pp. 349–363, Jan. 2016.

[13] R. Jiang, Z. Wang, Q. Wang, and L. Dai
Multi-user sum-rate optimization for visible light communications with lighting constraints
J. Lightw. Technol., vol. 34, no. 16, pp. 3943–3952, Aug. 2016.

[14] X. Zhang, Q. Gao, C. Gong, and Z. Xu
User grouping and power allocation for NOMA visible light communication multi-cell networks
IEEE Commun. Lett., vol. 21, no. 4, pp. 777–780, Apr. 2017.

[15] R. Jiang, Q. Wang, H. Haas, and Z. Wang
Joint user association and power allocation for cell-free visible light communication networks
IEEE J. Sel. Areas Commun., vol. 36, no. 1, pp. 136–148, Jan. 2018.

[16] X. Zhang, S. Dimitrov, S. Sinanovic, and H. Haas
Optimal power allocation in spatial modulation OFDM for visible light communications
In *Proc. IEEE 75th Veh. Technol. Conf.*, May 2012, pp. 1–5.

[17] Y. Xu *et al.*
Accuracy analysis and improvement of visible light positioning based on VLC system using orthogonal frequency division multiple access
Opt. Express vol. 25, no. 26, pp. 32618–32630, 2017.

[18] H. Yang, C. Chen, W. Zhong, A. Alphones, S. Zhang, and P. Du
Resource allocation for multi-user integrated visible light communication and positioning systems
In *Proc. IEEE Int. Conf. Commun.*, 2019, pp. 1–6.

[19] H. Yang, P. Du, W. Zhong, C. Chen, A. Alphones, and S. Zhang
Reinforcement learning-based intelligent resource allocation for integrated VLCP systems
IEEE Wireless Commun. Lett., vol. 8, no. 4, pp. 1204–1207, Aug. 2019.

[20] M. F. Keskin, A. D. Sezer, and S. Gezici
Optimal and robust power allocation for visible light positioning systems under illumination constraints
IEEE Trans. Commun., vol. 67, no. 1, pp. 527–542, Jan. 2019.

[21] K. Ying, H. Qian, R. J. Baxley, and S. Yao
Joint optimization of precoder and equalizer in MIMO VLC systems
IEEE J. Sel. Areas Commun., vol. 33, no. 9, pp. 1949–1958, Sep. 2015.

[22] H. Ma, L. Lampe, and S. Hranilovic
Coordinated broadcasting for multiuser indoor visible light communication systems
IEEE Trans. Commun., vol. 63, no. 9, pp. 3313–3324, Sep. 2015.

[23] P. J. Chung, H. Du, and J. Gondzio
A probabilistic constraint approach for robust transmit beamforming with imperfect channel information
IEEE Trans. Signal Process., vol. 59, no. 6, pp. 2773–2782, Jun. 2011.

[24] K. Y. Wang, T. H. Chang, W. K. Ma, A. M. C. So, and C. Y. Chi
Probabilistic SINR constrained robust transmit beamforming: A Bernstein-type inequality based conservative approach
In *Proc. IEEE Int. Conf. Acoust., Speech, Signal Process.*, May 2011, pp. 3080–3083.

[25] T. Wang, Y. Sekercioglu, A. Neild, and J. Armstrong
Position accuracy of time-of-arrival based ranging using visible light with application in indoor localization systems
J. Lightw. Technol., vol. 31, no. 20, pp. 3302–3308, Oct. 2013.

[26] M. F. Keskin and S. Gezici
Comparative theoretical analysis of distance estimation in visible light positioning systems
J. Lightw. Technol., vol. 34, no. 3, pp. 854–865, Feb. 2016.

[27] M. F. Keskin, S. Gezici, and O. Arikan
Direct and two-step positioning in visible light systems
IEEE Trans. Commun., vol. 66, no. 1, pp. 239–254, Jan. 2018.

[28] J. M. Kahn and J. R. Barry
Wireless infrared communications
Proc. IEEE, vol. 85, no. 2, pp. 265–298, Feb. 1997.

[29] E. F. Schubert
Light-Emitting Diodes. Cambridge, U.K.: Cambridge Univ. Press, 2003.

[30] Q. Li and W. K. Ma
Spatially selective artificial-noise aided transmit optimization for MISO multi-eves secrecy rate maximization
IEEE Trans. Signal Process., vol. 61, no. 10, pp. 2704–2717, May 2013.

[31] A. Nemirovski and A. Shapiro
Convex approximations of chance constrained programs
SIAM J. Opt., vol. 17, no. 4, pp. 969–996, 2006.

[32] W. W. L. Li, Y. J. Zhang, A. M. C. So, and M. Z. Win
Slow adaptive OFDMA systems through chance constrained programming
IEEE Trans. Signal Process., vol. 58, no. 7, pp. 3858–3869, Jul. 2010.

[33] K. Y. Wang, A. M. C. So, T. H. Chang, W. K. Ma, and C. Y. Chi
Outage constrained robust transmit optimization for multiuser MISO downlinks: Tractable approximations by conic optimization
IEEE Trans. Signal Process., vol. 62, no. 21, pp. 5690–5705, Nov. 2014.